Available online at www.sciencedirect.com
ScienceDirect
Journal of Power Sources 171 (2007) 917–921
JOURNAL OF POWER SOURCES
www.elsevier.com/locate/jpowsour

Short communication

Effect of carbon coating on $LiNi_{1/3}Mn_{1/3}Co_{1/3}O_2$ cathode material for lithium secondary batteries

Hyun-Soo Kim [a,*], Mingzhe Kong [a], Ketack Kim [a], Ick-Jun Kim [a], Hal-Bon Gu [b]

[a] *Korea Electrotechnology Research Institute, Changwon 641-120, Republic of Korea*
[b] *Chonnam National University, Gwangju 500-757, Republic of Korea*

Received 15 April 2007; received in revised form 28 April 2007; accepted 4 June 2007
Available online 21 June 2007

Abstract

Amorphous carbon is coated on $LiNi_{1/3}Mn_{1/3}Co_{1/3}O_2$ cathode material for lithium batteries. The carbon-coated material shows improved thermal stability and electrochemical performance compared with bare material.

Keywords: Carbon coating; Rate capability retention; Thermal stability; Lithium battery; Cathode material

1. Introduction

Lithium-ion batteries (LIB) have been widely used in portable appliances such as cellular phones, digital cameras and notebook PCs, because their performance is excellent, in particular they have high specific energy. Lithium cobalt dioxide has been being adopted as the cathode material in commercial LIBs, since it has many merits such as easy preparation, high electric conductivity, high specific energy, and stable discharge capacity. On the other hand, its low thermal stability and high cost are the main obstacles to its application in large-size cells for hybrid-electric vehicles. Recently, layer-structured $LiNiO_2$ and spinel-structured $LiMnO_2$ have been investigated as alternatives to $LiCoO_2$. $LiNiO_2$ has high reversible capacity but low thermal stability, and $LiMn_2O_4$ has high thermal stability and low cost but low reversible capacity. To overcome these disadvantages, much intensive research has been conducted on a new cathode material of $LiNi_{1/3}Mn_{1/3}Co_{1/3}O_2$. Ohzuku and Makimura [1] prepared a layer-structured $LiNi_{1/3}Mn_{1/3}Co_{1/3}O_2$ as the cathode material for a LIB, and this material has attracted attention as an alternative to $LiCoO_2$, because it has high capacity and a stable structure [1]. Furthermore, Amine et al. [2] reported that $LiNi_{1/3}Mn_{1/3}Co_{1/3}O_2$ is a promising candidate electrode materials for use in hybrid-electric vehicles. Its reversible capacity was measured to be 160 mAh g^{-1} at a cut-off voltage of 2.5–4.4 V, and was 200 mAh g^{-1} at a cut-off voltage of 2.8–4.6 V [3,4]. It has also been found [5] that $LiNi_{1/3}Mn_{1/3}Co_{1/3}O_2$ has a hexagonal α-$NaFeO_2$ crystal structure with a space group of $R\bar{3}m$ [5]. This material has, in comparison with $LiCoO_2$, a high thermal stability, and possesses excellent cell performance as well as being a relatively low-cost material. On the other hand, it has lower electronic conductivity than $LiCoO_2$ [6,7]. In order to improve the conductivity, there have been many studies relating to coating materials, such as Al_2O_3, $AlPO_4$, $LiAlO_2$ [8,9], applied to the surface of the material.

The aim of this work is to improve the rate capability of $LiNi_{1/3}Mn_{1/3}Co_{1/3}O_2$ by carbon coatings. Sugar is pyrolized to form a carbon layer on the active material. This layer can improve the charge-transfer rates for redox reactions.

2. Experimental

Table sugar was used to apply a carbon coating on the $LiNi_{1/3}Mn_{1/3}Co_{1/3}O_2$ surface. The $LiNi_{1/3}Mn_{1/3}Co_{1/3}O_2$ active material (Daejung Chemical Co.) was synthesized using a co-precipitation method. After preparing the sugar and the active material at a given ratio, they were mixed for 3 h using ethanol as the solvent. The mixed solution was sintered at 350 °C for 1 h in a box-type furnace. The coated carbon content was measured with a thermogravimetric analyzer (TGA, TA instruments, Q100) [6].

* Corresponding author. Tel.: +82 55 280 1663; fax: +82 55 280 1590.
E-mail address: hskim@keri.re.kr (H.-S. Kim).

0378-7753/$ – see front matter © 2007 Elsevier B.V. All rights reserved.
doi:10.1016/j.jpowsour.2007.06.028

In order to identify the crystal structure of $LiNi_{1/3}Mn_{1/3}Co_{1/3}O_2$ material, a PW1830 X-ray diffraction analyzer (Phillips Co.) was used. The sweep range (2θ) was set between 10° and 80°, and the step size was 0.02°. The surface structure and the ingredients of the obtained powder were analyzed by means of scanning electron microscopy (SEM) using a Hitachi S-4800 instrument. The surface morphologies were observed with an SEM (Philips XL 300) and a transmission electronic microscope (TEM, JEOL 2100F). The cathodes were prepared from an 86:6:8 (wt.%) mixture of active material; polyvinylidene difluoride (PVDF, Aldrich) as a binder and Super P carbon black (MMM Carbon) as conduction material. The mixed slurry was coated on an aluminum foil, dried at 100 °C for 24 h, and hot-roll pressed at a pressing ratio of 25%. Lithium metal and polypropylene (Asahi Co.) were used as an anode and a separator, respectively. A solution of EC/DEC (1:1 vol.%) with 1 M $LiPF_6$ was used as an electrolyte. A 2032-type coin cell was assembled in a dry room and aged for 24 h at normal temperature.

Differential scanning calorimetry (DSC) was used to determine the thermal stability of the active material. The analysis was undertaken with a DSC Q 1000 (TA Co.) instrument. The sample was made by charging the coin cell to 4.3 V versus Li/Li^+, and then drying it for 24 h at 80 °C. The temperature range for the measurement was between 50 and 500 °C, with a rate of increase of 10 °C min^{-1}.

In the rate performance tests, the cell was given a 30 min rest time after being charged at 0.2*C*, and its electrical discharge characteristics were evaluated by differentiating the discharge current at 0.2*C*, 0.5*C*, 1.0*C*, 2*C* and 5*C*, respectively. In the cycle performance test, after charging at 0.5*C* with a constant current, the cell was given 30 min rest time, and then discharged 100 times, repeatedly. The voltage range was between 2.8 and 4.3 V. Also, after 10 cycles, the electrical transmission rate was measured using IM6.

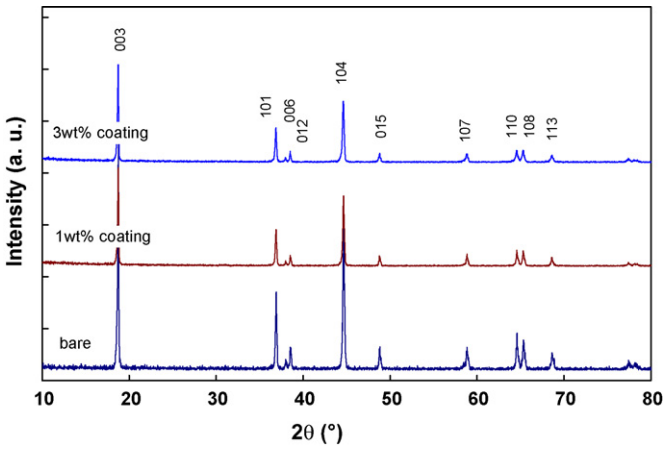

Fig. 1. X-ray patterns of bare- and carbon-coated $LiNi_{1/3}Mn_{1/3}Co_{1/3}O_2$ powder.

3. Results and discussion

The X-ray diffraction pattern of carbon-coated $LiNi_{1/3}Mn_{1/3}Co_{1/3}O_2$ active material is displayed in Fig. 1. Peaks due to the presence of impurities are not observed and the material has the hexagonal crystal structure of α-$NaFeO_2$ with a space group of

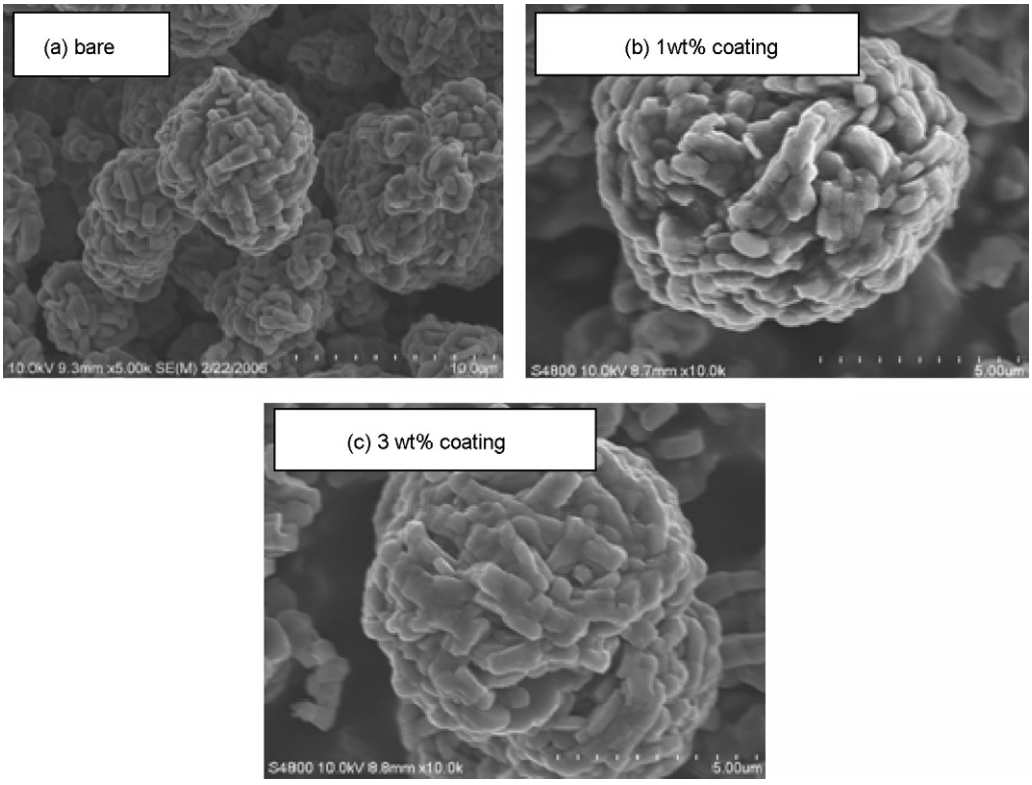

Fig. 2. SEM images of bare- and carbon-coated $LiNi_{1/3}Mn_{1/3}Co_{1/3}O_2$ powder.

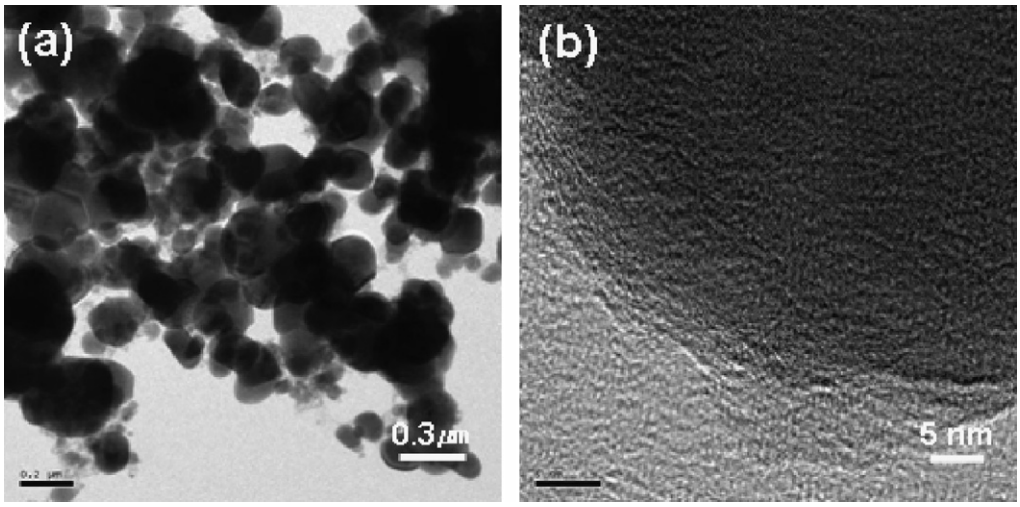

Fig. 3. TEM micrographs of carbon-coated $LiNi_{1/3}Mn_{1/3}Co_{1/3}O_2$ powder.

*R*3*m*. From the observation of peak splitting of 0 0 6/0 1 2 and 1 0 8/1 1 0 near 38° and 65°, respectively, it can be seen that the layered structure is well developed [5].

The surface morphologies of bare-, 1 and 3 wt.% carbon-coated active materials are given in Fig. 2. The $LiNi_{1/3}Mn_{1/3}Co_{1/3}O_2$ powders prepared by co-precipitation are not uniform in particle size. Small particles of 2–3 μm are clustered spherically in sizes ranging from 8 to 10 μm. However, the carbon-coated layer is not identifiable by SEM analysis. This is due to the fact that carbon is coated at a nano-thickness. Fig. 3 shows TEM images of carbon-coated $LiNi_{1/3}Mn_{1/3}Co_{1/3}O_2$ powders. It can be seen more clearly from the images that a nanolayer amorphous carbon is coated on the surface of $LiNi_{1/3}Mn_{1/3}Co_{1/3}O_2$ particles. Evidently, the nanolayer carbon is formed during the heat-treatment process. After milling in the planet mixer for a long time, the sugar is well-mixed with the $LiNi_{1/3}Mn_{1/3}Co_{1/3}O_2$ particles. With further calcination, the sugar decomposes into conductive carbon and coats on to the surfaces of $LiNi_{1/3}Mn_{1/3}Co_{1/3}O_2$ particles. Of course, the calcination time is an important factor. When the time is too long, the formed carbon will disappear due to reactions with oxygen in the air [10].

The thermal stability of the fully charged cell (4.3 V versus Li/Li^+) was measured using DSC. The results are shown in Fig. 4. There are two exothermic peaks for each sample. Usually, thermal decomposition properties are affected by the state of delithiation, synthesis method, preparation conditions, average particle size, size distribution, and type of electrolyte. The amount of heat generation of the non-coated sample is 161.3 J g^{-1} and the peak temperatures of the exothermic reaction are 362.4 and 457.8 °C, respectively. The two exothermic peaks of the 1 wt.% carbon-coated sample are somewhat different, although the initial heat generation is similar. The exothermic peaks of the 3 wt.% carbon-coated samples are greatly reduced compared with the bare sample; the peak temperatures are 379.8 and 456.5 °C and the heat generation is 105.8 J g^{-1}. It is concluded that the coated carbon layer on the particle surface of $LiNi_{1/3}Mn_{1/3}Co_{1/3}O_2$ active material suppresses the generation of oxygen and thus improves the thermal stability [11].

To evaluate the rate capability of the bare- and carbon-coated powder, the cells were charged and discharged at various cut-off voltages. The 1 wt.% carbon-coated sample was charged and discharged at a cut-off voltage of 2.8–4.3 V, and its voltage profile is shown in Fig. 5. Also, the discharge capacity and its retention of the bare-, 1 and 3 wt.% carbon-coated materials are summarized in Table 1. The bare material delivers a discharge capacity of 151.4 mAh g^{-1} at the 0.2*C* rate and 128.6 mAh g^{-1} at the 5*C* rate, i.e., a 84.9% retention of capacity compared to that at the 0.2*C*. The 1 wt.% carbon-coated sample exhibits a high discharge capacity of 134.3 mAh g^{-1} at the 5*C* rate, which is 87.4% discharge retention compared with the capacity of 153.7 mAh g^{-1} at the 0.2*C* rate. The rate performance of the 1 wt.% carbon-coated material is higher than that of $LiCoO_2$ coated with Al_2O_3; its capacity retention at the 1*C* rate is 91%

Table 1
Discharge capacity of bare- and carbon-coated $LiNi_{1/3}Mn_{1/3}Co_{1/3}O_2$ materials

Current rate	Bare		1 wt.% coating		3 wt.% coating	
	Discharge capacity (mAh g^{-1})	Capacity retention (%)	Discharge capacity (mAh g^{-1})	Capacity retention (%)	Discharge capacity (mAh g^{-1})	Capacity retention (%)
0.2*C*	151.4	100	153.7	100	144.6	100
0.5*C*	147.0	97.1	150.0	97.6	139.5	97.8
1*C*	141.2	93.3	145.7	94.8	132.3	92.8
2*C*	137.0	90.5	142.6	92.8	123.5	86.6
5*C*	128.6	84.9	134.3	87.4	113.2	79.4

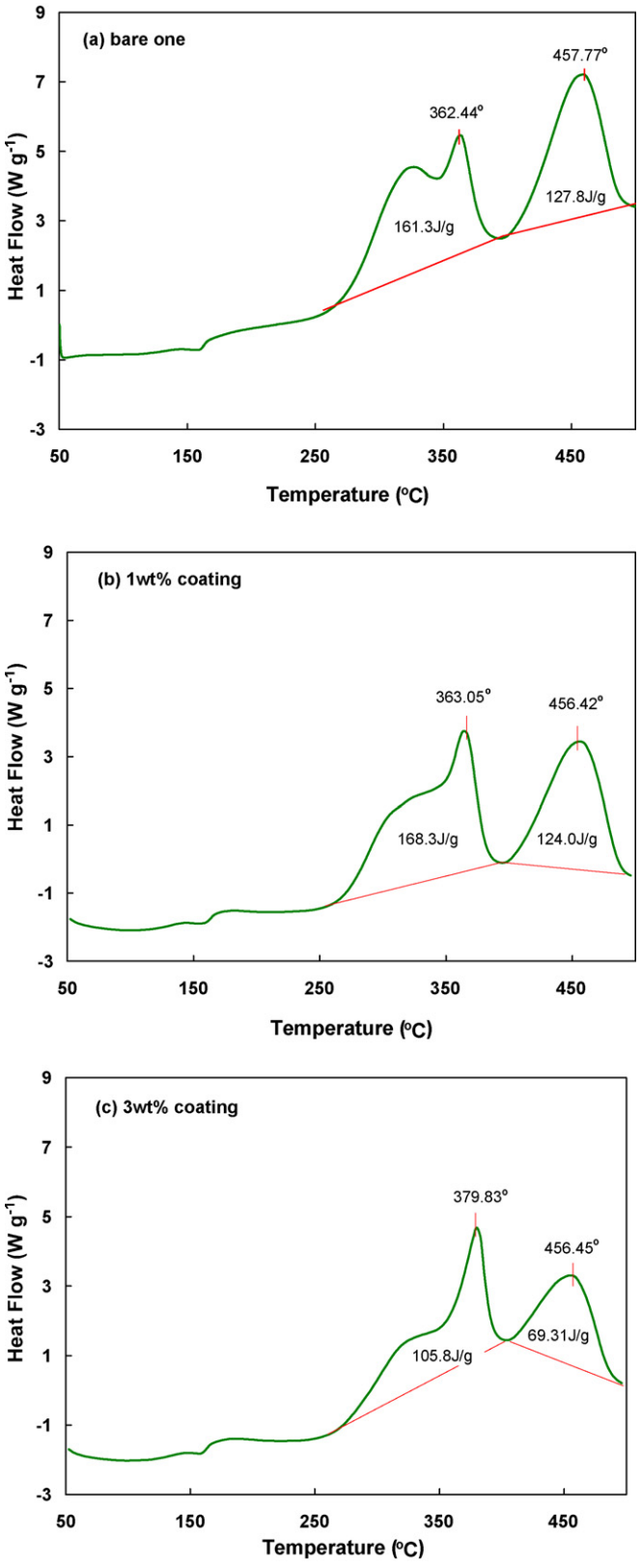

Fig. 4. DSC profiles of bare- and carbon-coated $LiNi_{1/3}Mn_{1/3}Co_{1/3}O_2$ powder after charging to 4.3 V.

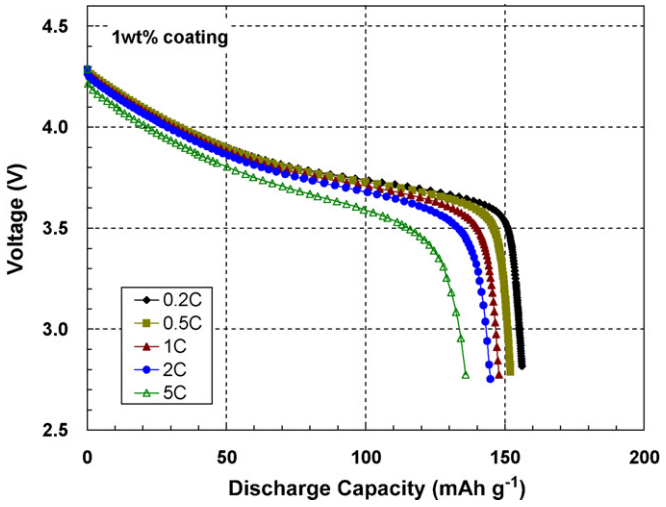

Fig. 5. Rate capability of 1 wt.% carbon-coated $LiNi_{1/3}Mn_{1/3}Co_{1/3}O_2$ materials.

compared with the 0.2*C* rate [12]. This is considered to be due to the fact that the electrical conductivity of the carbon-coated material has improved [13,14] and that this, in turn, has enhanced the rate performance. However, the 3 wt.% carbon-coated powder delivers a low discharge capacity of 113.2 mAh g^{-1} at the 5*C* rate, which is a capacity retention of 79.4% with respect to that at the 0.2*C* rate.

The $LiNi_{1/3}Mn_{1/3}Co_{1/3}O_2$ material was charged and discharged for 50 cycles, to evaluate its cycle life performance, over the voltage range of 2.8–4.3 V at the 0.5*C* rate. The discharge capacity of the sample as a function of cycle number is shown in Fig. 6. The capacity retention of the bare- and 1 wt.% carbon-coated material is similar after the 50th cycle, viz., 98%. By contrast, the capacity retention of the 3 wt.% carbon-coated sample decreases to 90% after 50 cycles. Furthermore, it is observed that after coating with carbon, the capacity is actually reduced. It is suggested that this might be due to the fact that inactive carbon materials are coated on the $LiNi_{1/3}Mn_{1/3}Co_{1/3}O_2$ material.

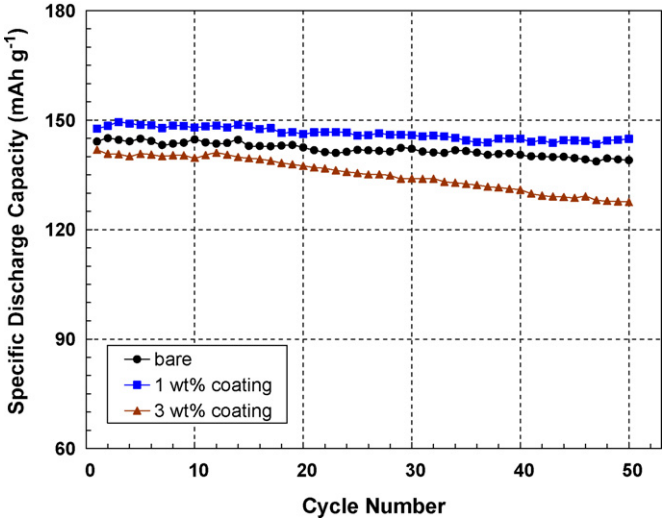

Fig. 6. Discharge capacity of bare- and carbon-coated $LiNi_{1/3}Mn_{1/3}Co_{1/3}O_2$ powder with charge–discharge cycling.

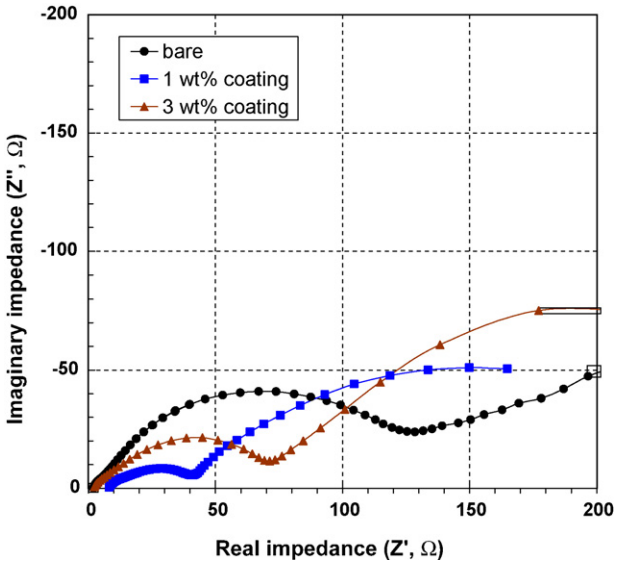

Fig. 7. Electrochemical impedance spectra of bare- and carbon-coated $LiNi_{1/3}Mn_{1/3}Co_{1/3}O_2$ materials after 10 charging–discharging cycles.

Typical Nyquist plots of the bare- and carbon-coated $LiNi_{1/3}Mn_{1/3}Co_{1/3}O_2$ composite electrodes are shown in Fig. 7. The impedance was measured after 10 cycles at the 0.5*C* rate over a voltage range between 2.8 and 4.3 V. Both types of material exhibit a semicircle in the high-frequency region, and a straight line in the low-frequency region. The numerical value of the semicircle diameter on the Z_{re} axis is approximately equal to the charge-transfer resistance (R_{ct}). After 1 wt.% carbon coating, R_{ct} is markedly decreased. The straight line is attributed to the diffusion of lithium ions into the bulk of the electrode material, which is called Warburg diffusion. After 10 cycles, the impedance of the bare material increases to 120 Ω, but the impedance of the 1 and 3 wt.% carbon-coated materials is actually reduced. The 1 wt.% carbon-coated sample shows the smallest impedance, viz., 40 Ω. This is probably because, the carbon coating has improved, the electric conductivity [15]. It is clear that the diffusion coefficient of the lithium ions is greatly increased during intercalation and de-intercalation by the carbon coating. This suggests that the carbon coating causes an enhancement of conductivity [16], which will be favourable for electrochemical performance during cycling at high rate.

4. Conclusions

Cells with the carbon-coated $LiNi_{1/3}Mn_{1/3}Co_{1/3}O_2$ active material have been prepared and their electrochemical characteristics have been evaluated. The following results have been obtained.

$LiNi_{1/3}Mn_{1/3}Co_{1/3}O_2$ material shows spherical morphology with an excellent layered structure. When carbon is coated on the particles via the addition of sugar, impurity peaks are not observed in XRD patterns. From DSC analysis, the carbon-coated layer on the surface of $LiNi_{1/3}Mn_{1/3}Co_{1/3}O_2$ active material is found to suppress the generation of oxygen and, in turn, improve thermal stability.

The rate capability of the material is improved by carbon coating of the material, compared with bare material; the capacity retention of a 1 wt.% carbon-coated sample at the 5*C* rate is 87.4% with respect to that at the 0.2*C* rate. After 50 charge–discharge cycles, the discharge capacity retention of the 1 wt.% carbon-coated material is 98%, i.e., similar to that of bare material.

References

[1] T. Ohzuku, Y. Makimura, Chem. Lett. 7 (2001) 642–643.
[2] G. Henriksen, K. Amine, J. Liu, P. Nelson, Abstract 255, 204th Meeting of the Electrochemical Society, Orlando, October 12–16, 2003.
[3] N. Yabuuchi, T. Ohzuku, J. Power Sources 119–121 (2003) 171–174.
[4] K.M. Shaju, G.V. Subba Rao, B.V.R. Chowdari, Electrochim. Acta 48 (2002) 145–151.
[5] J. Kim, C. Park, Y. Sun, Solid State Ionics 164 (2003) 43–49.
[6] H. Kim, J. Shin, S. Na, S. Eom, S. Moon, S. Kim, J. KIEEME 16 (2003) 994–1000.
[7] H. Kim, S. Kim, C. Lee, S. Moon, W. Kim, J. KIEEME 19 (2006) 139–144.
[8] Y. Kim, H. Kim, S.W. Martin, Electrochim. Acta 52 (2006) 1316–1322.
[9] H. Kim, S. Kim, S.W. Martin, J. Power Sources 161 (2006) 623–627.
[10] Q. Cao, H. Zhang, G. Wang, Q. Xia, Y. Wu, H. Wu, Electrochem. Commun. 9 (2007) 1228–1232.
[11] I. Belharouak, W. Lu, D. Vissers, K. Amine, Electrochem. Commun. 8 (2006) 329–335.
[12] H. Kweon, J. Park, J. Seo, G. Kim, B. Jung, H. Lim, J. Power Sources 126 (2004) 156–162.
[13] G. Wang, L. Yang, S. Bewlay, Y. Chen, H. Liu, J. Ahn, J. Power Sources 146 (2005) 521–524.
[14] B.L. Cushing, J.B. Goodneough, Solid State Sci. 4 (2002) 1487–1493.
[15] H. Shin, W. Cho, H. Jang, J. Power Sources 159 (2006) 1383–1388.
[16] H. Liu, C. Li, H. Zhang, L. Fu, Y. Wu, H. Wu, J. Power Sources 159 (2006) 717–720.